IJCSE International Journal of Computer Sciences and Engineering Open Access
Research Paper Volume-4, Issue-9 E-ISSN: 2347-2693

Mathematical Analysis of Robust Anisotropic Diffusion Filter for Ultrasound Images

Sumit Kushwaha

Electronics Engineering Department, Kamla Nehru Institute of Technology, Sultanpur, India.

Available online at: www.ijcseonline.org

Received: 19/Aug/2016 Revised: 29/Aug/2016 Accepted: 14/Sept/2016 Published: 30/Sep/2016

***Abstract*— Anisotropic Diffusion is very efficient non-linear image processing PDE based technique which simultaneously restore images and enhance image features for 2-D or, 3-D images. This technique is described by local eigenvalues and local eigenvectors of the anisotropic diffusion tensor field where anisotropic diffusion coefficients are depending on direction and position. Here, mathematical analysis of robust anisotropic diffusion (RAD) filter for ultrasound (US) image has been discussed in this paper. It includes probabilistic memory mechanism and speckle statistics models of tissues characterization and adapts the anisotropic diffusion tensor to the ultrasound image iteratively. Higher frequency absorbed by tissue and skin but cannot penetrate deeply in comparison to lower frequency which give poorer image quality by echo signals, so we get an inferior quality image with some clinical information loss. This clinical information loss is restored by iterative process of various state-of-the-art filters, but discussed RAD filter shows better performance in terms of measured MSE and SSIM index, with including memory mechanism and speckle statistics, and preserves the relevant tissue details for clinical purposes.**

Keywords: Ultrasound imaging, speckle filter, anisotropic diffusion, tensor, Volterra equations.

I. INTRODUCTION

Ultrasound (US) imaging technique is very popular imaging technique and plays an important role in real time diagnosis and treatment. It is a non-invasive nature, no emission of ionizing radiations, the low cost involved imaging technique. It is very helpful for many medical conditions such as cardiology, gynecology, neonatology, ophthalmology, orthopedics, etc. there are two types of US imaging system: two dimensional (2-D) and three dimensional (3-D) US imaging system. However, 2-D US imaging technique is conventional and having some limitations such as 2-D frame is produced at a given time (i.e. interest of structure of volume quantization in the body). In some medical conditions, structure of volume quantization (view area) is very important to find out the disease and its cure in advance. Thus, 3-D US imaging technique has drawn attention of researchers in recent years. Quantitative analysis and visual inspection are two different ways for 3-D US imaging data analyzing. Quantitative analysis can be manual or may be automatic that can be used for diagnosis to obtain some data/measurements. Usually, measurement of geometric distances and volumes comes under the quantitative analysis. Visual inspections are involved for real time diagnosis by the physician. The coherent nature of US imaging results with speckle noise which is multiplicative in nature, locally correlated noise, that reduces its utility for less than highly trained users and also complicates image processing task such as feature segmentation [15]. In some clinical applications, speckle reduction may be counterproductive. Therefore, many speckle reduction filters have been proposed. Speckle behavior in US images can be seen as a random process whose statistical features depend on the tissue class. [17] US imaging generally done between 2 to 18 MHz higher frequency range to get better image quality for clinical applications. Higher frequency absorbed by tissue and skin but cannot penetrate deeply in comparison to lower frequency which give poorer image quality by echo signals and speckle phenomena is inherent response of echo signals which provide important features for clinical purposes. Thus speckle noise removal filters are based on local statistics.

Many state-of-the-art filters try to minimize the poor resolution and maximize sharpening the boundary at edges likewise the behavior of non-homogeneous diffusive phenomena of heat. Among these state-of-the-art filters, we focus on an anisotropic diffusion filter [22] based on probabilistic memory mechanism and speckle statistics models of tissues characterization. We mathematically analyze a PDE based approach to speckle reducing anisotropic diffusion filter with application to B-Mode US image of human kidney which include probability model and adapt iteratively to the filtered image. For better boundary estimation and preservation of the clinical details for diagnostic purposes, probability model structure tensor, which belongs to each tissue in US image, defines a diffusion tensor for taking into consideration of the boundaries between different tissue classes for filtering purposes. In experiments and results section, we get better result in comparison to [22] after some modification in parameters selection. This is the main contribution of this work.

II. BACKGROUND

A. Specle Noise Model

Here, we represent $g(x,y,z)$ the degraded quality image, $n(x,y,z)$ the noise which degraded the quality of the image and introduced in image during acquisition process, $f(x,y,z)$ the original image (that we want to restore). During some image acquisition process such as MRI, additive noise introduced which is represented by Gaussian variable of zero mean and a given standard deviation. Mathematically, the additive noise degraded quality image $g(x,y,z)$ can be represented by [21]:

$$g(x,y,z) = f(x,y,z) + n(x,y,z) \quad (1)$$

And, during some image acquisition process such as US imaging, multiplicative noise, known as speckle, introduced which is represented by variable of mean and standard deviation. Mathematically, the speckle noise degraded quality image $g(x,y,z)$ can be represented by:

$$g(x,y,z) = f(x,y,z)n(x,y,z) + m(x,y,z) \quad (2)$$

where, $n(x,y,z)$ and $m(x,y,z)$ are multiplicative and additive noise component respectively. As, we see the effect of additive noise behavior is very small in compared to multiplicative noise behavior. So, we neglect the additive noise behavior in speckle noise, then simplified model which is mathematically expressed as:

$$g(x,y,z) = f(x,y,z)n(x,y,z) \quad (3)$$

In fact, an accurate description of the speckle noise pattern statistics is still an active research area which involves complex analytical modelling. Speckle noise behavior statistics can be categorized into different classes according to the number of scatterers per resolution cell (Scatterer Number Density (SND)) to their spatial distribution and to the characteristics of the imaging system [3].

B. Classical Filters

Many filters have been proposed and developed for minimization of speckle noise effect in imaging such as Synthetic Aperture Radar (SAR) images and US images. The LEE [1] and KUAN [2] filters have the same mathematical formulation but they differ in derivations and modelling assumption. Actually, both filters make an output image by using linear combination computing. They select average intensity window to get a center pixel intensity in filter window and by varying window size attain a balance between coefficient of variation (point feature, edge feature, diffusion in homogeneous region, etc.). FROST filter [4] attains a balance by varying coefficient of variation such that filter preserves image features if coefficient of variation is high and filter not preserves image features if coefficient of variation is low. However, existing edge preserving and feature preserving image restoration filters have major limitations such as shape of the filter and size of window. If window size is too large, edge will not preserve and over-filtering (smoothing) occur [5], [6]. Then, an outlined partial differential equation (PDE) based diffusion technique is introduced for reducing speckled noise. This PDE based approach preserve edges and image features also as same manner Perona and Malik anisotropic diffusion [7], [8], [9] and we explore the anisotropic diffusion application in speckle imagery fields such as SAR, medical imaging, etc.

C. Diffusion Filters for Speckle

Diffusion is a physical process to create equilibrium concentration differences without destroying or, creating body mass. This physical observation expressed equilibration property by Fick's law of diffusion equation [10]:

$$\frac{\partial u(x,y,z;t)}{\partial t} = \nabla.\left(D(x,y,z;t)\nabla u(x,y,z;t)\right)$$
$$= \frac{\partial}{\partial x}\left(D(x,y,z;t) \times \frac{\partial}{\partial x}u(x,y,z;t)\right)$$
$$+ \frac{\partial}{\partial y}\left(D(x,y,z;t) \times \frac{\partial}{\partial y}u(x,y,z;t)\right)$$
$$+ \frac{\partial}{\partial z}\left(D(x,y,z;t) \times \frac{\partial}{\partial z}u(x,y,z;t)\right) \quad (4)$$

with initial condition $u_0\ (x,y,z) = u(x,y,z;\ t=0)$ which is noisy image/input image. $u(x,y,z;t)$ is the output image. D is diffusion coefficient, known as symmetric positive definite tensor, which depend on local structure of $u(x,y,z;t)$ (if D is constant, then filter is isotropic diffusion filter and if D is not constant, then filter is anisotropic diffusion filter) and $\nabla.$ and ∇ denote the divergence operator and gradient operator, respectively, $u_0(x,y,z)$ is the initial image, i.e. noisy image, t is temporal variable. Eq. (4), Linear Anisotropic Diffusion (LAD), is an elliptic Partial Differential Equation (PDE). Here, $D: \Omega \rightarrow S_d^+$ is a given field of symmetric positive definite diffusion tensors where Ω is an open region of $\mathbb{R}^3$ and $\partial\Omega$ is boundary of Ω. Eigenvectors of these tensors define preferential diffusion directions, and the Eigenvalues their corresponding coefficients. Evolution rule eq. (4) is complemented with an initial condition $u(x,y,z;0) = u_0(x,y,z)$ at time t = 0. If $u_0(x,y,z)$ has pixels of vector type, then their components are treated independently [12].

By using finite difference method, eq. (4) given as:

$$\frac{\partial}{\partial x}\left(D(x,y,z;t) \times \frac{\partial}{\partial x}u(x,y,z;t)\right)$$

which is expressed as

$$\frac{\partial}{\partial x}\left(D(x,y,z;t) \times \frac{\partial}{\partial x}u(x,y,z;t)\right)$$
$$\approx \frac{\partial}{\partial x}\left\{D(x,y,z;t)\frac{1}{\Delta x}[u(x+\Delta x,y,z;t) - u(x,y,z;t)]\right\}$$
$$\approx$$
$$\frac{1}{\Delta x^2}\left\{\begin{matrix} D(x,y,z;t)\begin{bmatrix} u(x+\Delta x,y,z;t) - u(x,y,z;t) \\ -u(x,y,z;t) + u(x-\Delta x,y,z;t)\end{bmatrix} \\ + [D(x+\Delta x,y,z;t) - D(x,y,z;t)]\begin{bmatrix} u(x+\Delta x,y,z;t) \\ -u(x,y,z;t)\end{bmatrix}\end{matrix}\right\}$$
$$\approx \frac{1}{\Delta x^2}\left\{\begin{matrix} D(x+\Delta x,y,z;t)[u(x+\Delta x,y,z;t) - u(x,y,z;t)] \\ + D(x,y,z;t)[u(x-\Delta x,y,z;t) - u(x,y,z;t)]\end{matrix}\right\}$$

(5)

where "≈" shows that the R.H.S. part of the equation is the difference approximation of the L.H.S. part.

Similarly, we have

$$\frac{\partial}{\partial y}\left(D(x,y,z;t) \times \frac{\partial}{\partial y}u(x,y,z;t)\right)$$
$$\approx \frac{1}{\Delta y^2}\left\{\begin{matrix} D(x,y+\Delta y,z;t)[u(x,y+\Delta y,z;t) - u(x,y,z;t)] \\ + D(x,y,z;t)[u(x,y-\Delta y,z;t) - u(x,y,z;t)]\end{matrix}\right\}$$

(6)

and,

$$\frac{\partial}{\partial z}\left(D(x,y,z;t) \times \frac{\partial}{\partial z}u(x,y,z;t)\right)$$

$$\approx \frac{1}{\Delta z^2}\begin{Bmatrix} D(x,y,z+\Delta z;t)[u(x,y,z+\Delta z;t)-u(x,y,z;t)] \\ +D(x,y,z;t)[u(x,y,z-\Delta z;t)-u(x,y,z;t)] \end{Bmatrix}$$

(7)

All the values of eq. (5), eq. (6), and eq. (7) inserting in eq. (4) to obtain difference approximation of $\frac{\partial u(x,y,z;t)}{\partial t}$. Put Δx = 1, Δy = 1, and Δz = 1we get:

$$\frac{\partial u(x,y,z;t)}{\partial t} \approx \begin{Bmatrix} D(x+1,y,z;t)[u(x+1,y,z;t)-u(x,y,z;t)] \\ +D(x,y,z;t)[u(x-1,y,z;t)-u(x,y,z;t)] \end{Bmatrix} + \begin{Bmatrix} D(x,y+1,z;t)[u(x,y+1,z;t)-u(x,y,z;t)] \\ +D(x,y,z;t)[u(x,y-1,z;t)-u(x,y,z;t)] \end{Bmatrix} + \begin{Bmatrix} D(x,y,z+1;t)[u(x,y,z+1;t)-u(x,y,z;t)] \\ +D(x,y,z;t)[u(x,y,z-1;t)-u(x,y,z;t)] \end{Bmatrix}$$

(8)

So, obtaining discrete realization of anisotropic diffusion filter for $u(x,y,z;t)$ image from eq. (8):

$$u(x,y,z;t+1) = u(x,y,z;t) + \begin{Bmatrix} D(x+1,y,z;t)[u(x+1,y,z;t)-u(x,y,z;t)] \\ +D(x,y,z;t)[u(x-1,y,z;t)-u(x,y,z;t)] \end{Bmatrix} + \begin{Bmatrix} D(x,y+1,z;t)[u(x,y+1,z;t)-u(x,y,z;t)] \\ +D(x,y,z;t)[u(x,y-1,z;t)-u(x,y,z;t)] \end{Bmatrix} + \begin{Bmatrix} D(x,y,z+1;t)[u(x,y,z+1;t)-u(x,y,z;t)] \\ +D(x,y,z;t)[u(x,y,z-1;t)-u(x,y,z;t)] \end{Bmatrix}$$

(9)

In eq. (9), we can see that the major problem is selection of diffusion coefficient $D(x,y,z;t)$ in anisotropic diffusion filter.

Most of the diffusion filters are simply modifications of perona-malik filter [11] where D is constant (scalar coefficient based on gradient of the image $D\nabla u(x,y,z;t)$ which avoids diffusion near the boundaries and applies it in homogeneous areas). To create a speckle imagery affected smooth region [13] propose a new anisotropic diffusion filter Speckle reducing anisotropic diffusion (SRAD). SRAD selects finite power intensity image $u_0(x,y,z)$ and having none zero-valued intensities over the image domain Ω, and we get the output image $u(x,y,z;t)$ by following PDE:

$$\begin{cases} \frac{\partial u(x,y,z;t)}{\partial t} = \nabla.[C(q)\,\nabla u(x,y,z;t)] \\ u(x,y,z;0) = u_0(x,y,z) \\ \left.\frac{\partial u(x,y,z;t)}{\partial \vec{n}}\right|_{\partial\Omega} = 0 \end{cases} \quad (10)$$

where $\partial\Omega$ denotes the boundary of Ω, $\vec{n}$ is the outer normal to the $\partial\Omega$, and $C(q)$ is coefficient of diffusion which is defined as a decreasing function of the instantaneous coefficient of variation. Eq. (10) is known as SRAD PDE.

$$C(q) = \frac{1}{1+\frac{q^2(x,y,z;t)-q_0^2(t)}{q_0^2(t)[1+q_0^2(t)]}} \quad (11)$$

or,

$$C(q) = \exp\left[-\left\{\frac{q^2(x,y,z;t)-q_0^2(t)}{q_0^2(t)(1+q_0^2(t))}\right\}\right] \quad (12)$$

In eq. (11) and (12), $q(x,y,z;t)$ is the instantaneous coefficient of variation serves as the edge detector in speckled imagery, $q_0(t)$ is the speckle scale function and is estimation parameter related to the coefficient of variation of noise. $q(x,y,z;t)$ is determined by:

$$q(x,y,z;t) = \sqrt{\frac{\frac{1}{3}\left(\frac{|\nabla u(x,y,z;t)|}{u(x,y,z;t)}\right)^2 - \left(\frac{1}{6}\right)^2\left(\frac{\nabla^2 u(x,y,z;t)}{u(x,y,z;t)}\right)^2}{\left[1+\left(\frac{1}{6}\right)\left(\frac{\nabla^2 u(x,y,z;t)}{u(x,y,z;t)}\right)\right]^2}} \quad (13)$$

In case of 2-D, instantaneous coefficient of variation $q(x,y;t)$:

$$q(x,y;t) = \sqrt{\frac{\frac{1}{2}\left(\frac{|\nabla u(x,y;t)|}{u(x,y;t)}\right)^2 - \left(\frac{1}{4}\right)^2\left(\frac{\nabla^2 u(x,y;t)}{u(x,y;t)}\right)^2}{\left[1+\left(\frac{1}{4}\right)\left(\frac{\nabla^2 u(x,y;t)}{u(x,y;t)}\right)\right]^2}} \quad (14)$$

Let us consider how to obtain $q(x,y,z;t)$, we know:

$$C^2_{(i,j,k)} = \frac{\left[u^2_{(i,j,k)} + \frac{1}{|W|}\nabla^2 u^2_{(i,j,k)}\right]}{\left[u_{(i,j,k)} + \frac{1}{|W|}\nabla^2 u_{(i,j,k)}\right]^2} - 1 \quad (15)$$

In continuous domain, we have [13]:

$$\nabla^2 u^2_{(i,j,k)} = 2\left|\nabla u_{(i,j,k)}\right|^2 + 2u_{(i,j,k)}(\nabla^2 u_{(i,j,k)}) \quad (16)$$

Eq. (16) represented as follow in discrete domain:

$$\nabla^2 u^2_{(i,j,k)} = \left|\nabla_1 u_{(i,j,k)}\right|^2 + \left|\nabla_2 u_{(i,j,k)}\right|^2 + 2u_{(i,j,k)}(\nabla^2 u_{(i,j,k)}) \quad (17)$$

where $\nabla_1 u_{(i,j,k)}$ and $\nabla_2 u_{(i,j,k)}$ obtained by:

$$\nabla_1 u_{(i,j,k)} = \begin{bmatrix} u_{i,j,k} - u_{(i-1,j,k)}, u_{(i,j,k)} \\ -u_{(i,j-1,k)}, u_{(i,j,k)} - u_{(i,j,k-1)} \end{bmatrix} \quad (18)$$

$$\nabla_2 u_{(i,j,k)} = \begin{bmatrix} u_{(i+1,j,k)} - u_{(i,j,k)}, u_{(i,j+1,k)} \\ -u_{(i,j,k)}, u_{(i,j,k+1)} - u_{(i,j,k)} \end{bmatrix} \quad (19)$$

Let $\left|\nabla u_{(i,j,k)}\right|^2$ be discretized as the average of $\left|\nabla_1 u_{(i,j,k)}\right|^2$ and $\left|\nabla_2 u_{(i,j,k)}\right|^2$ and put the values of eq. (18) and eq. (19) into eq. (15), then we get:

$$C^2_{(i,j,k)} = \frac{\left[\frac{1}{3}|\nabla u_{(i,j,k)}|^2 - \frac{1}{36}(\nabla^2 u_{(i,j,k)})^2\right]}{\left[u_{(i,j,k)} + \frac{1}{6}\nabla^2 u_{(i,j,k)}\right]^2} \quad (20)$$

$C_{(i,j,k)}$ denoting the special case which computed over $|W|$ by $q_{(i,j,k)}$ then $q_{(i,j,k)}$ can be viewed as a discretization of:

$$q(x,y,z;t) = \sqrt{\frac{\frac{1}{3}\left(\frac{|\nabla u(x,y,z;t)|}{u(x,y,z;t)}\right)^2 - \left(\frac{1}{6}\right)^2\left(\frac{\nabla^2 u(x,y,z;t)}{u(x,y,z;t)}\right)^2}{\left[1+\left(\frac{1}{6}\right)\left(\frac{\nabla^2 u(x,y,z;t)}{u(x,y,z;t)}\right)\right]^2}} \quad (21)$$

As we see, SRAD filter is based on the filter originally proposed by [1]. Specially [1] starts from a linear approximation of eq. (3):

$$u_0(x,y,z) \approx \overline{n(x,y,z)}\, u(x,y,z;t) + \overline{u(x,y,z;t)}\,[n(x,y,z) - \overline{n(x,y,z)}] \quad (22)$$

where $\overline{u(x,y,z;t)}$ is mean of original image, $n(x,y,z)$ is speckle noise component present in noisy image, $\overline{n(x,y,z)}$ is noise mean, and $\sigma^2_{n(x,y,z)}$ is noise variance. Here, it supposed that noise mean and noise variance are constant throughout the noisy image.

As noted by [8] using eq. (11) is equivalent to a discrete version of the equation $\nabla.((1-k_L)\nabla u(x,y,z;t))$.

$$1 - k_L = 1 - \frac{v_{u(x,y,z;t)}}{v_{u(x,y,z;t)} + \sigma^2_{n(x,y,z)}\,\overline{u_0(x,y,z)^2}} = \frac{\sigma^2_{n(x,y,z)}\,\overline{u_0(x,y,z)^2}}{v_{u(x,y,z;t)} + \sigma^2_{n(x,y,z)}\,\overline{u_0(x,y,z)^2}} \quad (23)$$

$$= \frac{C^2_{n(x,y,z)}}{\left[\frac{\left(C^2 - C^2_{n(x,y,z)}\right)}{\left(1+C^2_{n(x,y,z)}\right)}\right] + C^2_{n(x,y,z)}} \quad (24)$$

$$= \frac{1}{1+\frac{\left(C^2 - C^2_{n(x,y,z)}\right)}{\left[C^2_{n(x,y,z)}\left(1+C^2_{n(x,y,z)}\right)\right]}} \quad (25)$$

The equivalent Kuan's filter is:

$$1 - k_K = 1 - \frac{v_{u(x,y,z;t)}}{v_{u_0(x,y,z)}} = \frac{1+\frac{1}{C^2}}{1+\frac{1}{C^2_{n(x,y,z)}}} \quad (26)$$

where, $v_{u_0(x,y,z)}$ is local variance of $u_0(x,y,z)$, $v_{u(x,y,z;t)}$ is the local spatial variance of $u(x,y,z;t)$ at current pixel (/voxel) location, $k_K = \frac{v_{u(x,y,z;t)}}{v_{u_0(x,y,z)}}$ is edge magnitude parameter, $k_L = \frac{v_{u(x,y,z;t)}}{v_{u(x,y,z;t)} + \sigma^2_{n(x,y,z)}\,\overline{u_0(x,y,z)^2}}$ is also edge magnitude parameter. This is the only difference between Kaun filter and Lee filter i.e. to change $k_L\ to\ k_K$ in the diffusion equation. $C^2_{(x,y,z)} = C^2 = \frac{v_{u_0(x,y,z)}}{\overline{u_0(x,y,z)^2}}$ is diffusion coefficient. $C^2_{n(x,y,z)} = \frac{\sigma^2_{n(x,y,z)}}{\overline{n(x,y,z)^2}}$, is diffusion coefficient of noise. Here, $q(x,y,z;t)$ is the discrete approximation of C and $q_0(t)$ the discrete approximation of $C_{n(x,y,z)}$ which need to estimate at each iteration.

D. Mathematical Application of SRAD Filter Algorithm

Here, four stage iterative method can be used to solve mathematically eq. (10). Let anisotropic diffusion time step Δt and spatial step h in x,y,z directions respectively, then the discretization of time and space coordinates as $t = n\Delta t;\ n = 0,1,2,3,\ldots\ldots$ and $x = ih, y = jh, z = kh; i = 0,1,2,3,\ldots\ldots,M-1, j = 0,1,2,3,\ldots,N-1, k = 0,1,2,3,\ldots\ldots, K-1$ respectively, where $Mh \times Nh \times Kh$ is support image size. Let $u^n_{(i,j,k)} = u(ih, jh, kh; n\Delta t)$, then iterative method can be described as:

1) Computing Laplacian Approximation and Derivative Approximation

$$\nabla_1 u^n_{(i,j,k)} = \left[\frac{u^n_{(i+1,j,k)} - u^n_{(i,j,k)}}{h}, \frac{u^n_{(i,j+1,k)} - u^n_{(i,j,k)}}{h}, \frac{u^n_{(i,j,k+1)} - u^n_{(i,j,k)}}{h}\right] \quad (27)$$

$$\nabla_2 u^n_{(i,j,k)} = \left[\frac{u^n_{(i,j,k)} - u^n_{(i-1,j,k)}}{h}, \frac{u^n_{(i,j,k)} - u^n_{(i,j-1,k)}}{h}, \frac{u^n_{(i,j,k)} - u^n_{(i,j,k-1)}}{h}\right] \quad (28)$$

$$\nabla^2 u^n_{(i,j,k)} = \frac{u^n_{(i+1,j,k)} + u^n_{(i-1,j,k)} + u^n_{(i,j+1,k)} + u^n_{(i,j-1,k)} + u^n_{(i,j,k+1)} + u^n_{(i,j,k-1)} - 6u^n_{(i,j,k)}}{h^2} \quad (29)$$

Here, we are using symmetric boundary conditions. So:

$$u^n_{(-1,j,k)} = u^n_{(0,j,k)}, u^n_{(M-1,j,k)} = u^n_{(M,j,k)};$$
$$j = 0,1,2,3\ldots, N-1; k = 0,1,2,3,\ldots, K-1 \quad (30)$$

$$u^n_{(i,-1,k)} = u^n_{(i,0,k)}, u^n_{(i,N-1,k)} = u^n_{(i,N,k)};$$
$$i = 0,1,2,3\ldots, M-1; k = 0,1,2,3,\ldots, K-1 \quad (31)$$

$$u^n_{(i,j,-1)} = u^n_{(i,j,0)}, u^n_{(i,j,K-1)} = u^n_{(i,j,K)};$$
$$i = 0,1,2,3\ldots, M-1; j = 0,1,2,3,\ldots, N-1 \quad (32)$$

2) Computing the Coefficient of Diffusion $C(q)$

$$C^n_{(i,j,k)} = C\left[q\left(\frac{1}{u^n_{(i,j,k)}}\sqrt{\left|\nabla_1 u^n_{(i,j,k)}\right|^2 + \left|\nabla_2 u^n_{(i,j,k)}\right|^2}, \frac{1}{u^n_{(i,j,k)}}\nabla^2 u^n_{(i,j,k)}\right)\right] \quad (33)$$

3) Computing $\nabla.[C(q)\,\nabla u(x,y,z;t)]$

Direction $d$at location (x,y,z):

$$d^n_{(i,j,k)} = \frac{1}{h^2}\begin{bmatrix} C^n_{(i+1,j,k)}\left(u^n_{(i+1,j,k)} - u^n_{(i,j,k)}\right) \\ +C^n_{(i,j,k)}\left(u^n_{(i-1,j,k)} - u^n_{(i,j,k)}\right) \\ +C^n_{(i,j+1,k)}\left(u^n_{(i,j+1,k)} - u^n_{(i,j,k)}\right)\end{bmatrix} + \frac{1}{h^2}\begin{bmatrix} C^n_{(i,j,k)}\left(u^n_{(i,j-1,k)} - u^n_{(i,j,k)}\right) \\ +C^n_{(i,j,k+1)}\left(u^n_{(i,j,k+1)} - u^n_{(i,j,k)}\right) \\ +C^n_{(i,j,k)}\left(u^n_{(i,j,k-1)} - u^n_{(i,j,k)}\right)\end{bmatrix} \quad (34)$$

with symmetric boundary condition.

$$d^n_{(-1,j,k)} = d^n_{(0,j,k)}, d^n_{(M-1,j,k)} = d^n_{(M,j,k)};$$
$$j = 0,1,2,3\ldots, N-1; k = 0,1,2,3,\ldots, K-1 \quad (35)$$

$$d^n_{(i,-1,k)} = d^n_{(i,0,k)}, d^n_{(i,N-1,k)} = d^n_{(i,N,k)};$$
$$i = 0,1,2,3\ldots, M-1; k = 0,1,2,3,\ldots, K-1 \quad (36)$$

$$d^n_{(i,j,-1)} = d^n_{(i,j,0)}, d^n_{(i,j,K-1)} = d^n_{(i,j,K)};$$
$$i = 0,1,2,3\ldots, M-1; j = 0,1,2,3,\ldots, N-1 \quad (37)$$

4) Mathematical Approximation to Differential Equation

$$u_{(i,j,k)}^{n+1} = u_{(i,j,k)}^{n} + \frac{\Delta t}{6}\, d_{(i,j,k)}^{n} \quad (38)$$

Eq. (38) is known as SRAD update function. For mathematical applications we choose $h = 1$, and $\Delta t = 0.05$.

E. Anisotropic Diffusion Flux (ADF)

The ADF equation can be written as:

$$\begin{cases} u(x,y,z;0) = u_0(x,y,z) \\ \frac{\partial u(x,y,z;t)}{\partial t} = \nabla . F(x,y,z;t) + \beta[u_0(x,y,z) - u(x,y,z;t)] \end{cases} \quad (39)$$

where $F(x,y,z;t)$ is the diffusion flux and β is a data attachment coefficient. If β = 0, then eq. (39):

- Heat diffusion flux $F(x,y,z;t) = \nabla u(x,y,z;t)$ which is equivalent to Gaussian convolution.
- Heat diffusion flux $F(x,y,z;t) = D(x,y,z;t)\nabla u(x,y,z;t)$ (from eq. (4)). High gradient diffusion effect reduced by use of this function which is based on a threshold value δ on gradient norm.

Diffusion matrix D proposed in [10] can be expressed in a diagonal form with Eigenvectors $\langle v_1, v_2, v_3 \rangle$ and Eigenvalues $(\lambda_1,\ \lambda_2, \lambda_3)$. So, Heat diffusion flux $F(x,t)$ can be expressed as:

$$F(x,y,z;t) = D\ \nabla u(x,y,z;t) = \sum_{i=1}^{3} \lambda_i\, u(x,y,z;t)_{v_i}\, v_i \quad (40)$$

where $u(x,y,z;t)_{v_i} = \nabla u(x,y,z;t) v_i$ is the 1st order derivative of the intensity in the direction of v_i. Author [14] uses a particular heat diffusion flux that is decomposed in the basis of the of the gradient $\langle v_1 \rangle$ (direction of the gradient), and the maximal $\langle v_2 \rangle$ and minimal $\langle v_3 \rangle$ curvature directions computed on the Gaussian smoothed image $u^*(x,y,z;t)$, here, smoothness is obtained by convolution of $u(x,t)$ with a Gaussian kernel $G_{N-D}(\vec{x},\sigma) = \frac{1}{(\sqrt{2\pi}\,\sigma)^N}\, e^{-\frac{|\vec{x}|^2}{2\sigma^2}}$ of standard deviation σ > 0, where D for dimensions, $N \in \mathbb{R}^n, n = 1,2,3, \ldots$ and $\vec{x} \in x, y, z \ldots$.

The principle curvature directions are acquired as the two eigenvectors of the matrix $PH_\sigma P$, where H_σ is Hessian Matrix of Gaussian smoothed image $u^*(x,y,z;t)$ and P is projection matrix, in the plane orthogonal to the gradient direction. Along with the direction of Eigenvector $< v_1 >$, to apply smoothing, the filter must preserve the boundaries and detect an edge clearly.

$$P = I - \left(\frac{\nabla u^*(x,y,z;t)}{|\nabla u^*(x,y,z;t)|}\right) \cdot \left(\frac{\nabla u^*(x,y,z;t)}{|\nabla u^*(x,y,z;t)|}\right)^t \quad (41)$$

where I is Identity matrix.

F. Anisotropic Diffusion Filter for Matrix Extension

SRAD filter is efficiently perform directional filtering after adding a non-scalar component to the filter. This SRAD filter do directional filtering of the image along the image structures for better result in restoration of images [15]. Formally, SRAD is written as:

$$\frac{\partial u(x,y,z;t)}{\partial t} = \nabla . [(1 - k_K)\, \nabla \mathrm{u}(x,y,z;t)]$$

$$= \nabla . \left(\begin{bmatrix} (1-k_K) & 0 & 0 \\ 0 & (1-k_K) & 0 \\ 0 & 0 & (1-k_K) \end{bmatrix} \nabla \mathrm{u}(x,y,z;t) \right) \quad (42)$$

From eq. (42), diffusion matrix $D = [(1 - k_K)\, I]$ is a scalar component matrix where I is Identity matrix. As we know that anisotropic diffusion flux F uses the direction of gradient and direction of principal curvature for a kind of sharper image. The combination of enhancement in the gradient direction with smoothing in the minimal curvature direction can lead very good enhancement of tubular structures like blood-vessels in 3D images [15]. On the basis of Eigenvectors $\langle v_1, v_2, v_3 \rangle$ and Eigenvalues $(\lambda_1,\ \lambda_2, \lambda_3)$ new diffusion matrix can be written as: λ_1 as $(1 - k_K(x,y,z))$ and fixed λ_2 to constant C_{max} and fixed λ_3 to C_{min}. In case of anisotropic diffusion flux F, we use $C_{max} \ll C_{min}$. For example, we use $C_{max} = 0$ and $C_{min} = 1$. So, filtered image $\mathrm{u}(x,y,z;t)$ with OSRAD filter:

$$D = (v_1|\ v_2\ |v_3) \begin{pmatrix} (1 - k_K(x,y,z)) & 0 & 0 \\ 0 & C_{max} & 0 \\ 0 & 0 & C_{min} \end{pmatrix} \begin{pmatrix} v_1^T \\ v_2^T \\ v_3^T \end{pmatrix} \quad (43)$$

where C_{max} is the amount of smoothing along the direction of maximal curvature, and C_{min} is the amount of smoothing along the direction of minimal curvature. In case of 2-D images, the parameter C_{max} and C_{min} reduces to just one coefficient C_{tang}.

G. PDE model Volterra Filter

Authors [16] proposed a new type of non-linear anisotropic diffusion equation for regularization of PDEs. This new type of non-linear anisotropic diffusion equation was combined with a time-delay. The PDE model:

$$\frac{\partial u(x,y,z;t)}{\partial t} - \nabla . \big(L(x,y,z;t) \nabla u(x,y,z;t)\big) = 0 \quad (44)$$

$$\frac{\partial L(x,y,z;t)}{\partial t} + L(x,y,z;t) = F(x,y,z;t)\big(\nabla_\sigma\, u(x,y,z;t)\big) \quad (45)$$

where $\nabla_\sigma\, u(x,y,z;t) = \nabla(u(x,y,z;t) * G_{\sigma\, N-D}(\vec{x},\sigma))$, $G_{\sigma\, N-D}(\vec{x},\sigma) = \frac{G_{N-D}\left(\frac{\vec{x},\sigma}{\sigma}\right)}{\sigma^2}$, $\int G_{N-D}(\vec{x},\sigma) d\Omega = 1$. $G_{N-D}(\vec{x},\sigma)$ is Gaussian kernel used in bounded region for smoothness. $L(x,y,z;t)$ is the diffusion tensor at point (x,y,z) and time t. For well-posedness of this system model, σ is used as positive smoothing parameter ($\nabla_\sigma = \nabla, if\ \sigma = 0$). So, eq. (44) and (45) after combined with time-delay, the equations becomes:

$$\frac{\partial u(x,y,z;t)}{\partial t} - \nabla . \big(L(x,y,z;t) \nabla u(x,y,z;t)\big) = 0 \quad (46)$$

$$\frac{\partial L(x,y,z;t)}{\partial t} + \frac{L(x,y,z;t)}{\tau} = \frac{F(x,y,z;t)(\nabla_\sigma\, u(x,y,z;t))}{\tau} \quad (47)$$

where τ is time delay (relaxation time). This temporal dependence due to the coupling with delay differential equation (DDE) used in non-linear anisotropic diffusion equation for regularization of PDEs in eq. (47).

The system with initial conditions i.e. t = 0 such as noisy image $u_0(x,y,z)$, initial diffusion tensor $L_0(x,y,z;0) = L_0(x,y,z)$ and periodic boundary conditions. For processing of images, boundary conditions are not essential task. Avoiding boundary conditions, by part integrations met in the result and filtered image is considered as the steady solution of eq. (46) and (47), so, stopping time is avoided. The Volterra equation:

$$\frac{\partial u(x,y,z;t)}{\partial t} - e^{-t}\nabla.\{L_0(x,y,z)\nabla_\sigma u(x,y,z;t)\} - \int_0^t e^{\Omega-t}\nabla.\{F(x,y,z;t)[\nabla_\sigma u(x,y,z,\Omega)]\nabla_\sigma u(x,y,z;t)\}\,d\Omega = 0 \quad (48)$$

The Volterra equation with time delay τ:

$$\frac{\partial u(x,y,z;t)}{\partial t} - e^{-\frac{t}{\tau}}\nabla.\{L_0(x,y,z)\nabla_\sigma u(x,y,z;t)\} - \int_0^t e^{\frac{(\Omega-t)}{\tau}}\nabla.\{F(x,y,z;t)[\nabla_\sigma u(x,y,z,\Omega)]\nabla_\sigma u(x,y,z;t)\}\,d\Omega = 0 \quad (49)$$

III. Robust Anisotropic Diffusion Filtering

The novelty of this filtering technique is to eliminate the effect of gradient information due to the lack of contours and low contrast of US images with objective of preservation of relevant clinical details in interest region using probabilistic-driven selective memory mechanism filtering. A new selective filtering tensor operator $O(x,y,z;t)$ used as transformation of the instantaneous diffusion tensor $D(x,y,z;t)$ at location (x,y,z) into a null tensor for suitable tissue characterization and preservation. In this context, $p(x,y,z;t) = 1 - \overline{p(x,y,z;t)}$ where, $p(x,y,z;t)$ for the probability of the tissue regions and $\overline{p(x,y,z;t)}$ for the probability of the non-tissue (meaningless) regions. For this selective behavior the diffusion tensor $D(x,y,z;t)$ is multiplied by its Eigenvalues by $\overline{p(x,y,z;t)}$. Memory mechanism used, to know the anisotropic diffusion direction satisfy the condition that $\overline{p(x,y,z;t)} \to 0$, so $\tau(x,y,z)\,\overline{p(x,y,z;t)} \to \infty$. Memory mechanism will be disable if $\overline{p(x,y,z;t)} \to 1$, so that $\tau(x,y,z)\,\overline{p(x,y,z;t)} \to 0$. So the new reconstruct diffusion tensor by using expansion of outer product:

$$O\big(D(x,y,z;t)\big) = E(x,y,z;t)S\,E(x,y,z;t)^T \quad (50)$$

where

$$S = \frac{1}{\overline{p(x,y,z;t)}}\begin{pmatrix}\lambda_1(x,y,z;t) & 0 & 0\\ 0 & \lambda_2(x,y,z;t) & 0\\ 0 & 0 & \lambda_3(x,y,z;t)\end{pmatrix}$$

and $E(x,y,z;t) = (v_1|\,v_2\,|v_3)$ and $E(x,y,z;t)^T = \begin{pmatrix}v_1^T\\ v_2^T\\ v_3^T\end{pmatrix}$.

Preserving pathway of the time dependent probability for getting more robust characterization than obtained from instantaneous probability, $\overline{p(x,y,z;t)}$, tensor operator $O(x,y,z;t)$ is not directly applied to $L(x,y,z;t)$. This $\overline{p(x,y,z;t)}$ provides more robust characterization than $\overline{p(x,y,z;t)}$.

Now, our proposed system DDE, with same initial and periodic condition as [15] and $\tau(x,y,z)$ is the spatial dependence of τ, will be:

$$\frac{\partial u(x,y,z;t)}{\partial t} = \nabla.\big(L(x,y,z;t)\big)\,\nabla u(x,y,z;t) \quad (51)$$

$$\frac{\partial L(x,y,z;t)}{\partial t} = \frac{L(x,y,z;t)}{\tau(x,y,z)} - O(D(x,y,z;t)) \quad (52)$$

Integrate eq. (52), we get:

$$L(x,y,z;t) = O\big(D(x,y,z;0)\big)e^{\frac{-t}{\tau(x,y,z)}} + \int_0^t e^{\frac{(\Omega-t)}{\tau(x,y,z)}}O\big(D(x,y,z,\Omega)\big)\,d\Omega \quad (53)$$

To turn ON/OFF the memory mechanism, spatial dependence $\tau(x,y,z)$ should satisfied the minimum conditions that $\tau(x,y,z)$: $[0,1] \to (0,\infty)$. The anisotropic diffusion flux $F(x,y,z;t) = L(x,y,z;t)\nabla u(x,y,z;t)$, then from eq. (53):

$$F(x,y,z;t) = F_1(x,y,z;t) + F_2(x,y,z;t) \quad (54)$$

where filtered diffusion tensor $O\big(D(x,y,z,\Omega)\big)$, $\Omega \le t$, $F^{(t,\Omega)}(x,y,z) = O\big(D(x,y,z,\Omega)\big)\nabla u(x,y,z;t)$ and

$$F_1(x,y,z;t) = O\big(D(x,y,z,0)\big)e^{\frac{-t}{\tau(x,y,z)}}\nabla u(x,y,z;t) = e^{\frac{-t}{\tau x,y,z}}F^{(t,0)}(x,y,z) \quad (55)$$

$$F_2(x,y,z;t) = \int_0^t e^{\frac{(\Omega-t)}{\tau(x,y,z)}}O\big(D(x,y,z,\Omega)\big)\,\nabla u(x,y,z;t)\,d\Omega = \int_0^t e^{\frac{(\Omega-t)}{\tau(x,y,z)}}F^{(t,\Omega)}(x,y,z)\,d\Omega \quad (56)$$

IV. Experiments and Results

A. Images

We consider the 'true' B-Mode US image of human kidney presented in [18] are used in this experiment. This real US image is used for quantitative analysis. The size of the 'true' B-Mode US image of human kidney is 522x469x24 (in pixel unit) in x, y, and z directions respectively.

B. Performance Metrics

Two performance metrics were used in our experiments to measure the algorithm performance, one is called Mean Squared Error (MSE) which is used for accuracy and precision of the 'true' image and other is called Structural Similarity Index Measure (SSIM) which is used for quality similarity between two images (original image and filtered image).

1) Mean Squared Error

The MSE is beneficial to have some measure of the difference between a pair of similar images. The most common difference measure is the mean-square error [19]. The MSE measure is popular because it correlates practical image with reference image for visually qualify test and MSE is mathematically tractable. Let $u(x,y,z;0)$ be pixel value intensity of reference image at (x,y,z) and measured image $u(x,y,z;t)$ at (x,y,z) coordinate axis. The MSE is defined as:

$$MSE = \frac{1}{MNK}\sum_{x=0}^{M-1}\sum_{y=0}^{N-1}\sum_{z=0}^{K-1}(|u(x,y,z;t) - u(x,y,z;0)|^2)$$

(57)

2) Structure Similarity Index Measure

SSIM which is based on human visual system is proposed by [20]. They argue that natural image signals are highly structured as the nearby pixels exhibits strong dependencies. SSIM is a function of three components: luminance comparison, contrast comparison, and structure comparison. Mathematically it can be written as:

$$SSIM\ (p,q) = [l(p,q)]^{\alpha}[c(p,q)]^{\beta}[s(p,q)]^{\gamma} \quad (58)$$

where p and q are the original and distorted image contents at the local window respectively. $\alpha, \beta, and\ \gamma$ are parameters that adjust the relative significance of the three components.

The luminance comparison function l is given by:

$$l(p,q) = \frac{2(1+R)}{1+(1+R)^2+\frac{C_1}{\mu_p^2}} \quad (59)$$

where $C_1 = (K_1, L)^2$, with L being the dynamic range of the pixel values and $K_1 << 1$ is a small constant. R being a measure of luminance change relative to background luminance that incorporates Weber's law. Mean intensity of signal p is represented by μ_p.

The contrast comparison function is defined as:

$$c(p,q) = \frac{(2\sigma_p\sigma_q+C_2)}{(\sigma_p^2+\sigma_q^2+C_2)} \quad (60)$$

Here, $C_2 = (K_2, L)^2$ and $K_2 << 1$. σ_p and σ_q are the standard deviations of signals p and q respectively.

The structural comparison function is given as:

$$s(p,q) = \frac{\sigma_{pq}+C_3}{\sigma_p\sigma_q+C_3} \quad (61)$$

where C_3 is a constant and σ_{pq} is the correlation coefficient of signals p and q. If $\alpha = \beta = \gamma = 1$ and $C_3 = \frac{C_2}{2}$, then:

$$SSIM(p,q) = \frac{(2\mu_p\mu_q+C_1)(2\sigma_{pq}+C_2)}{(\mu_p^2+\mu_q^2+C_1)(\sigma_p^2+\sigma_q^2+C_2)} \quad (63)$$

C. Result for Real US Image

In this section, we show the performance of RAD filter with real US image in order to compare with other state-of-the-art algorithms, discussed in background section. We consider the 'true' B-Mode US image presented in [18]. Designing of optimized RAD filter is very careful precision task which highly depend on anisotropic diffusion step, Δt, and iterations number, $n_{iteration}$. W related to filter window size, $\sigma_{u(x,y,z;t)}$ related to the structure diffusion tensor (smoothing parameter for derivatives), $\rho_{u(x,y,z;t)}$ smoothing parameter for anisotropic diffusion tensor, c_{tang} related to amount of anisotropic diffusion along the orthogonal direction to edges. We keep $\rho_{u(x,y,z;t)} = \sigma_{u(x,y,z;t)}$ for optimization purpose. Both numerical validation MSE and SSIM was used to measure the performance of state-of-the-art filters and discussed RAD filters respectively. Discussed RAD filter preserves the clinical details while performing filtering of US image. The image presented in Fig. 1(a). shows a B-mode US image of an anatomic phantom of a human kidney, Fig.1(b). is speckled image with standard deviation σ = 0.4, and Fig.1(h). shows RAD filtered image. The performance response of state-of-the-art filters is visually shown from Fig.1(c). to Fig.1(g). and comparative response of all mentioned filters is given in table - II. The optimization criterion for all filters given in table -I.

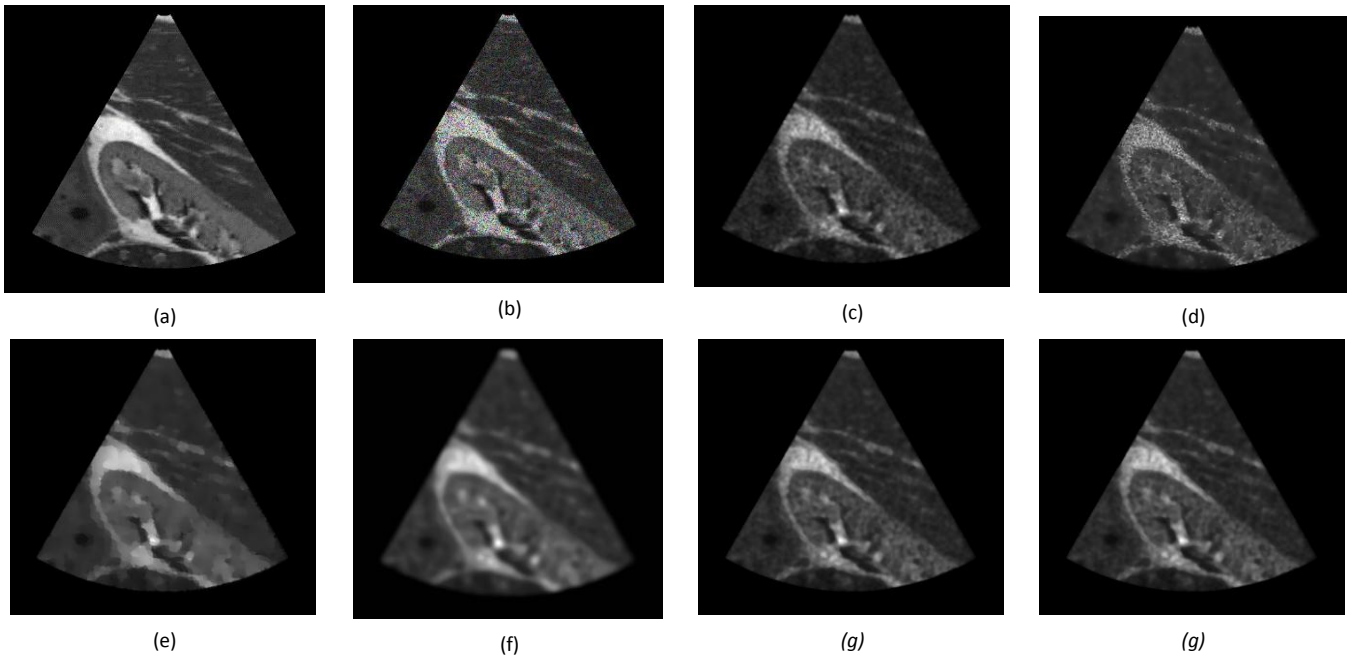

Figure 1. Experimental results obtained for real B-mode US image of human kidney; (a) original image, (b) speckle image with σ = 0.4, (c) FROST filter, (d) SRAD filter, (e) DPAD filter, (f) OSRAD filter, (g) POSRAD filter, (h) RAD filter.

Figure 2. Optimized Parameters Criterion for the filtering real B-mode US image of human kidney

Filter	*Optimized Parameters*
FROST Filter	$W = 7$
SRAD Filter	$\Delta t = 0.3, n_{iteration} = 80$
DPAD Filter	$\Delta t = 0.3, W = 2, n_{iteration} = 30$
OSRAD Filter	$\Delta t = 0.3, \sigma_{u(x,y,z;t)} = 4, c_{tang} = 15, n_{iteration} = 78$
POSRAD Filter	$\Delta t = 0.3,\ \sigma_{u(x,y,z;t)} = 4,\ \ \rho = 4, n_{iteration} = 26$
RAD Filter	$\Delta t = 0.2, \sigma_{u(x,y,z;t)} = 1, \rho_{u(x,y,z;t)} = 1, n = 30, n_{iteration} = 55$

Figure 3. MSE and SSIM Results on filtering real B-mode US image of human kidney

S.No.	*Filter*	*MSE*	*SSIM*
1.	Noisy Image	0.0145	0.7216
2.	FROST Filter	0.0035	0.8450
3.	SRAD Filter	0.0185	0.7635
4.	DPAD Filter	0.0040	0.8892
5.	OSRAD Filter	0.0025	0.8651
6.	POSRAD Filter	0.0024	0.8827
7.	RAD Filter	0.0020	0.8931

V. CONCLUSIONS

This paper presents a mathematical analysis of RAD filter for speckle noise reduction in real B-Mode US images on the basis of the performance evaluation metrics. We have used two performance metrics MSE and SSIM for which state-of-the-art filters gives optimum results but they suppress desired clinical tissue details when dealing with real US images. Here, DDE which is used in Volterra equation, implemented as memory mechanism. The performance comparison, shown in table – I and table – II, shows that discussed RAD filter gives better results, after some modification in parameters selection, in comparison to state-of-the-art filters and preserves the relevant tissue details for clinical purpose with including memory mechanism. This methodology offers an advantage over the discussed state-of-the-art filters in each iteration while preserving and enhancing the tissue details and gives better result for US image restoration. Future work includes improving of the RAD filter by taking into the account for more complex and real imaging images with speckle distribution.

REFERENCES

[1] J.-S. Lee, "Digital image enhancement and noise filtering by use of local statistics," IEEE Trans. Pattern Anal. Mach. Intell., vol. PAMI-2, no. 2, pp. 165–168, Mar. 1980.

[2] D. T. Kuan, A. A. Sawchuk, T. C. Strand, and P. Chavel, "Adaptive noise smoothing filter for images with signal-dependent noise," IEEE Trans. Pattern Anal. Mach. Intell., vol. PAMI-7, no. 2, pp. 165–177, Mar. 1985.

[3] K. Krissian, C.-F. Westin, R. Kikinis, and K. G. Vosburgh, "Oriented speckle reducing anisotropic diffusion," IEEE Trans. Image Process., vol. 16, no. 5, pp. 1412–1424, May 2007.

[4] V. Frost, J. Stiles, K. Shanmugan, and J. Holzman, "A model for radar images and its application to adaptive digital filtering of multiplicative noise," IEEE Trans. PAMI, vol. 4, no. 2, pp. 157–166, 1982.

[5] S. Gupta, R. Chauhan, and S. Sexana, "Wavelet-based statistical approach for speckle reduction in medical ultrasound images." Med Biol Eng Comput, vol. 42, no. 2, pp. 189–92, Mar 2004.

[6] L. Rudin, P.-L. Lions, and S. Osher, "Multiplicative denoising and deblurring: Theory and algorithms," in Geometric Level Set Methods in Imaging, Vision and Graphics. Springer-Verlag, 2003, ch. 6, pp. 103–120.

[7] Y. Yu and S. Acton, "Edge detection in ultrasound imagery using the instantaneous coefficient of variation," IEEE Transactions on Image Processing, vol. 13, no. 12, pp. 1640–1655, 2004.

[8] S. Aja-Fern´andez and C. Alberola-L´opez, "On the estimation of the coefficient of variation for anisotropic diffusion speckle filtering," IEEE Transactions on Image Processing, in press, vol. 15, no. 9, pp. 2694– 2701, sep 2005.

[9] K. Z. Abd-Elmoniem, A.-B. M. Youssef, and Y. M. Kadah, "Real-time speckle reduction and coherence enhancement in ultrasound imaging via nonlinear anisotropic diffusion," IEEE Trans Biomed Eng, vol. 49, no. 9, pp. 997–1014, Sep 2002.

[10] J. Weickert, Anisotropic Diffusion in Image Processing. Stuttgart, Germany: Teubner, 1998.

[11] P. Perona and J. Malik, "Scale-space and edge detection using anisotropic diffusion," IEEE Trans. Pattern Anal. Mach. Intell., vol. 12, no. 7, pp. 629–639, Jul. 1990.

[12] Jean-Marie Mirebeau, Jer^ome Fehrenbach, Laurent Risser, and Shaza Tobji,"Anisotropic Diffusion in ITK", arXiv: 1503.00992v1 [cs.CV], March, 2015.

[13] Y. Yu and S. T. Acton, "Speckle reducing anisotropic diffusion," IEEE Trans. Image Process., vol. 11, no. 11, pp. 1260–1270, Nov. 2002.

[14] K. Krissian, "Flux-based anisotropic diffusion applied to enhancement of 3d angiogram," IEEE Trans. Medical Imaging, vol. 21, no. 11, pp. 1440–1442, Nov. 2002.

[15] K. Krissian, C.-F. Westin, R. Kikinis, and K. G. Vosburgh, "Oriented speckle reducing anisotropic diffusion," IEEE Trans. Image Process., vol. 16, no. 5, pp. 1412–1424, May 2007.

[16] G. H. Cottet and M. E. Ayyadi, "A Volterra type model for image processing," IEEE Trans. Image Process., vol. 7, no. 3, pp. 292–303, Mar. 1998.

[17] F. Destrempes, J. Meunier, M. F. Giroux, G. Soulez, and G. Cloutier, "Segmentation in ultrasonic B-mode images of

healthy carotid arteries using mixtures of Nakagami distributions and stochastic optimization," IEEE Trans. Med. Imag., vol. 28, no. 2, pp. 215–229, Feb. 2009.

[18] Jorgen Arendt Jensen's website, http://field-ii.dk/ for Field – II Simulation Program.

[19] M. Nachtegeal, "Fuzzy techniques in image processing", volume 52, SPRINGER-Verlag, New York, 2000.

[20] Z. Wang, A. C. Bovik, H. R. Sheikh, and E. P. Simoncelli, "Image Quality Assessment: From error visibility to structural similarity", IEEE Transaction on Image Processing, 13(3), pp. 1 – 14, March 2000.

[21] Sumit Kushwaha and Rabindra Kumar Singh, "Study of Various Image Noises and their Behaviors", International Journal of Computer Sciences and Engineering (IJCSE), vol. 3, issue 3, March 2015, E-ISSN: 2347-2693.

[22] G. Ramos-Llordén, G. Vegas-Sánchez-Ferrero, M. Martin-Fernandez, C. Alberola-López and S. Aja-Fernández, "Anisotropic Diffusion Filter With Memory Based on Speckle Statistics for Ultrasound Images," in IEEE Transactions on Image Processing, vol. 24, no. 1, pp. 345-358, Jan. 2015.

Author Profile

Sumit Kushwaha pursed Bachelor of Technology from Uttar Pradesh Technical University, Lucknow, India in 2009 and Master of Technology from Sam Higginbottom Institute of Agriculture, Technology and Sciences, Allahabad, India in year 2012. He is currently pursuing Ph.D. and currently working as Research-cum-Teaching Fellow in Department of Electronics Engineeing, Kamla Nehru Institute of Technology, Sultanpur, India since 2014. He has 3 years of teaching experience.

